

Fluctuations and Higgs mechanism in Under-Doped Cuprates : a Review

C. Pépin,¹ D. Chakraborty,¹ M. Grandadam,¹ and S. Sarkar¹

¹*Institut de Physique Théorique, Université Paris-Saclay, CEA, CNRS, F-91191 Gif-sur-Yvette, France.*

The physics of the pseudo-gap phase of high temperature cuprate superconductors has been an enduring mystery in the past thirty years. The ubiquitous presence of the pseudo-gap phase in under-doped cuprates suggests that its understanding holds a key in unraveling the origin of high temperature superconductivity. In this paper, we review various theoretical approaches to this problem, with a special emphasis on the concept of emergent symmetries in the under-doped region of those compounds. We differentiate the theories by considering a few fundamental questions related to the rich phenomenology of these materials. Lastly we discuss a recent idea of two kinds of entangled preformed pairs which open a gap at the pseudo-gap onset temperature T^* through a specific Higgs mechanism. We give a review of the experimental consequences of this line of thoughts.

The Pseudo-Gap (PG) state of the cuprates was discovered in 1989 [1], three years after the discovery of high temperature superconductivity in those compounds. It was first observed in nuclear magnetic resonance (NMR) experiments, in an intermediate doping regime $0.06 < p < 0.20$, as a loss of the density of states at the Fermi level [1–3] at temperatures above the superconducting transition temperature T_c . Subsequently, angle resolved photo emission spectroscopy (ARPES) established that a part of the Fermi surface is gapped in the Anti-Nodal Region (ANR) (regions close to $(0, \pm\pi)$ and $(\pm\pi, 0)$ points) of the Brillouin zone, leading to the formation of Fermi ‘arcs’. Though the PG state shows behaviors of a metal, the appearance of Fermi ‘arcs’ instead of a full Fermi surface results into the violation of the conventional Luttinger theorem of Fermi liquid theory. Furthermore, surface spectroscopies like ARPES (see e.g. [4–8]) and scanning tunneling spectroscopy [9–11] show that the magnitude of the anti-nodal (AN) gap is unchanged when entering the superconducting (SC) phase below T_c (see Fig. 1a). The PG state persists up to a temperature T^* which decreases linearly with doping. The AN gap is also visible in two-body spectroscopy, for example in the B_{1g} channel of Raman scattering [12–14], which shows that below T_c , the pair breaking gap of superconductivity follows the T^* line with doping, in good agreement with the AN gap observed in ARPES. In contrast to the SC phase, the PG state is found to be independent of disorder or magnetic field. Despite of numerous invaluable experimental and theoretical investigations over the last three decades, various puzzles of the PG state remains to be solved.

In this paper, we review three different theoretical per-

spectives to the PG state of cuprate superconductors. We then focus on one specific theoretical approach where fluctuations protected by a specific Higgs mechanism are held responsible for the unusual properties of the pseudo-gap phase.

1. MOTT PHYSICS AND STRONGLY CORRELATED ELECTRONS

An overall glance at the phase diagram of the cuprate superconductors shows that superconductivity sets up close to an anti-ferromagnetic (AF) phase transition, but also close to a Mott insulating phase (Fig. 2). The presence of the metal-insulating transition so close to superconductivity is unusual and led many theoreticians to attribute the PG phase to a precursor of the Mott transition (a few review papers [15–24]). The Coulomb interaction has a high energy scale $U = 1eV$ which prohibits the double occupancy on each site and induces strong correlations between electrons. An effective Hamiltonian can be derived by integrating out formally the Coulomb interaction, which leads to AF super-exchange interaction associated with a constraint prohibiting double occupancy on each site for conduction electrons (see e.g. [16, 25, 26]) and is given by

$$H = \sum_{i,j} t_{ij} c_{i\sigma}^\dagger c_{j\sigma} + J \sum_{\langle i,j \rangle} \mathbf{S}_i \cdot \mathbf{S}_j, \quad (1)$$

where $c_{i,\sigma}^\dagger$ ($c_{i,\sigma}$) is a creation (annihilation) operator for an electron at site i with spin σ , $\mathbf{S}_i = c_{i,\alpha}^\dagger \boldsymbol{\sigma}_{\alpha,\beta} c_{i,\beta}$ is the spin operator at site i ($\boldsymbol{\sigma}$ is the vector of Pauli matrices), $t_{ij} = t_{ji}$ and J is the spin-exchange interaction. No double occupancy constraint is ensured by taking $n_i \leq 1$ with $n_i = \sum_{\sigma} c_{i,\sigma}^\dagger c_{i,\sigma}$ being the number operator. Theories then associate the formation of the PG phase as a precursor of the Mott transition, involving some fractionalization of the electron due to the constraint $n_i \leq 1$. The typical and simplest realization of such a program is to consider that the electron fractionalizes into “spinons” ($f_{i\sigma}^\dagger$) and “holons” (b_i) subject to a local U(1) or gauge symmetry group,

$$c_{i\sigma}^\dagger = f_{i\sigma}^\dagger b_i, \quad (2)$$

where $f_{i\sigma}^\dagger$ is the creation operator for a fermion carrying the spin of the electron, b_i is the annihilation operator for a boson carrying the charge. The no double occupancy constraint $n_i \leq 1$ is replaced by an equality

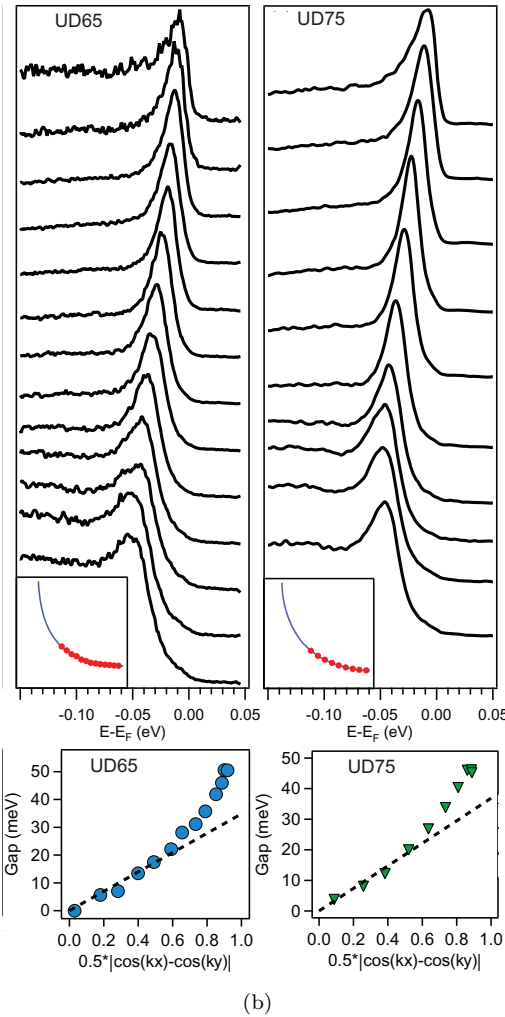
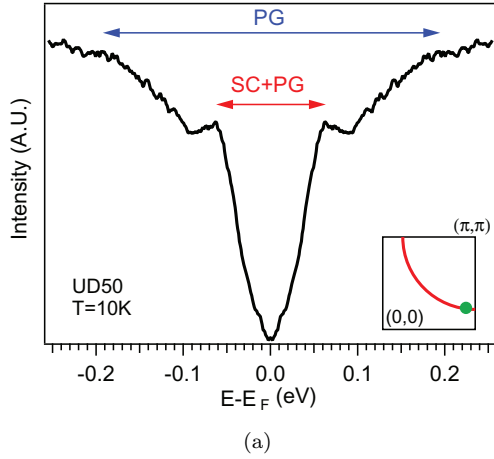


FIG. 1: a) The anti-nodal gap measured by ARPES spectroscopy, which shows two gaps, the first energy scale correspond to the PG scale E^* whereas the second energy scale corresponds to the spectroscopic gap E_{spec}^* . The data have been symmetrized with respect to the energy E_F . b) Two sets of ARPES lines scanning the Fermi surface of Bi1221 in the under-doped region. One sees that the quasi-particle peak at $E = 0$ present in the nodal region (the upper curves) evolves into a Bogoliubov quasi-particle peak at finite E in the anti-nodal region (the lower curves). One can see how the Bogoliubov peak in the anti-nodal region is still visible, whereas somewhat broadened. Data taken from Ref. [7]

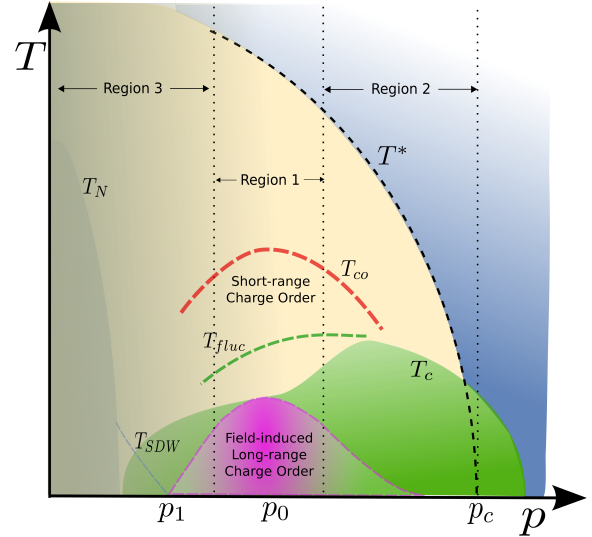


FIG. 2: The schematic phase diagram of cuprates superconductors as a function of hole doping [35]. On the left hand side, for $0 < p < 0.06$, the system has an AF phase. The Green region below T_c denotes the superconducting state. Below T_{co} the short range charge order is observed, whereas the purple region is the charge order observed with application of a magnetic field. T^* is represented with a dashed line which encloses the PG phase marked with yellow. In Region 3 and Region 2 we have additional source of damping, respectively due to the approach of the Mott transition and the proximity to the PG quantum critical point.

constraint

$$\sum_{\sigma} f_{i\sigma}^{\dagger} f_{i\sigma} + b_i^{\dagger} b_i = 1, \quad (3)$$

which is enforced using a Lagrange multiplier [27]. In this formalism, $\sum_{i\sigma} f_{i\sigma}^{\dagger} f_{i\sigma}$ gives the total fermion density and $\sum_i b_i^{\dagger} b_i$ gives the total holon density. The invariance under the charge conjugation, $f_{i\sigma}^{\dagger} \rightarrow e^{i\theta_i} f_{i\sigma}^{\dagger}$ and $b_i \rightarrow e^{-i\theta_i} b_i$ is implemented through the constraint in Eq. 3. Other ways of fractionalizing the electrons of course exist, with the celebrated Z_2 gauge theory leading to “visons” excitations [28, 29], or with extensions to higher groups like the pseudo-spin group $SU(2)$ [30, 31] or the spin group $SU(2)$ [32–34].

In all these cases the fractionalization of the electron into various entities is effective in the ANR of the Brillouin zone, opening a PG through the formation of small hole pockets. In this framework, the global understanding of the phase diagram (as a function of doping) goes in the following way (see Fig. 3a). A first line increasing with doping, describes the Bose condensation of the holons. Implicit is the assumption that the system is three dimensional so that the Bose condensation T_b occurs at finite temperature. A second line T^* decreasing with doping describes the PG phase and is typically as-

sociated to a precursor of pairing. For example in the U(1) theory, the T^* line corresponds to the condensation of spinon pairs $\langle f_{i\sigma}^\dagger f_{j\sigma}^\dagger \rangle$ on a bond. Strong coupling theories of the PG with electron fractionalization can be considered as various examples of the celebrated Resonant Valence Bond (RVB) theory [36] introduced in the early days after the discovery of cuprates, where some sort of spin liquid associated with fluctuating bond states is considered as the key ingredient for the formation of the PG [37, 38]. When the two lines cross, below T^* and T_b the electron re-confines so that the SC transition is also a confining transition from the gauge theory perspective. Above is the strange metal (SM) phase (Region IV) whereas on the right we find the typical metallic- Landau Fermi liquid phase (Region I).

Although this line of approach has been supported by a huge body of theoretical work, we are skeptical that this is the final solution for the PG phase. First, fractionalization of the electron produces, when it happens, very spectacular effects like the quantization of the resistivity, observed for example in the theory of fractional Quantum Hall Effect (QHE). Here no spectroscopic signature of “reconfinement” of the electron has been observed at finite energy. Moreover, in most of the under-doped region of cuprates, the ground state is a superconductor. If the electron fractionalize at T^* and that the ground state is a superconductor, it means that at T_c the electron shall re-confine, form the Cooper pairs and globally freeze the phase of the Cooper pairs. Of course it is possible but quite unlikely. A key experiment which illustrates this feature is maybe ARPES measurements which shows the presence of Bogoliubov quasi-particle in the ANR of the Brillouin zone, in the under-doped region inside the SC phase (see e.g. [7]). Taken at its face value this experience clearly hints at the formation of the SC state on the *whole* Fermi surface, including the ANR, rather than on small hole pockets centered around the nodes (see Fig.1b). In this paper, we will now focus on the two other avenues of investigations which are the fluctuations and the hidden phase transition at T^* .

2. PHASE FLUCTUATIONS

The realization that phase fluctuations are important in the under-doped region of the cuprates stems back from the seminal paper by Emery and Kivelson, which pointed out that close to a Mott transition, the localization of the electrons induces strong phase fluctuations of all the fields present in the system [40]. The origin of these fluctuations is deep and comes from the Heisenberg uncertainty principle, in which the particle/wave duality ensures that the localization of particles in space will generate phase fluctuations. Careful study of the penetration depth as a function of doping shows that cuprates are in the class of superconductors where the phase of the Cooper pairs strongly fluctuates at T_c lead-

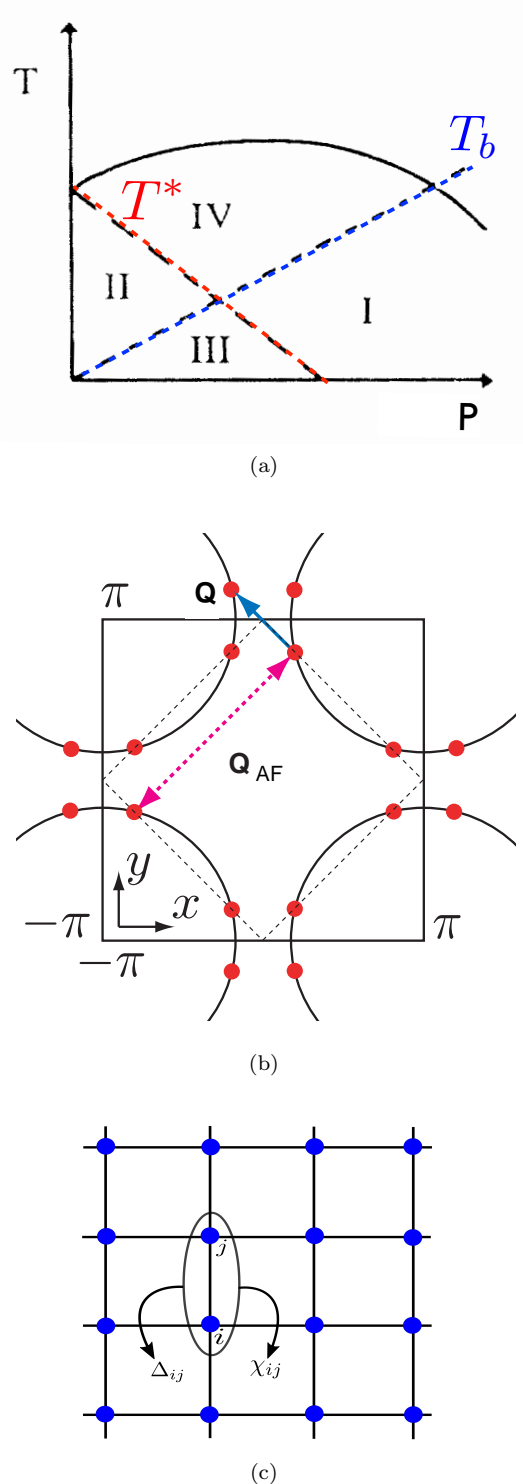


FIG. 3: a) The phase diagram from strong coupling theories. The first line, below which the Bose condensations (“holons”) occurs, and the second line, below which sees the formation of “spinon-spinon” pairing, cross each other resulting into formation of a spin liquid or “Resonating Valence Bond” (RVB) state. b) Schematic picture of the eight hot spots (EHS) model. The dots in red are the eight hot spots. The diagonal modulation wave vector is shown in blue (from Ref. [39]) c) Schematic depiction of bond variables on a square lattice.

ing to a Berezinsky Kosterlitz Thouless transition typical of strong 2D fluctuations (see e.g. [41, 42]). Early experiments showed a linear dependence between the T_c and the penetration depth, giving a lot of impetus to the fluctuations scenario [43, 44].

Another phenomenology which can be successfully explained by phase fluctuations of the Cooper pairs, lies in spectroscopic studies of the spectral gap associated to the transition at T^* . Surface spectroscopies like STM and ARPES tell us that the magnitude of the spectral gap associated to the PG, which lies in the ANR of the Brillouin zone, is unchanged when one goes through the SC T_c [45, 46], whereas the gap broadens more and more until T^* . On the other hand, in the nodal region, the spectral gap vanishes at T_c as it should within the standard BCS theory. Moreover, we learn from Raman scattering spectroscopies that in the B_{1g} channel, which scans the ANR, the spectral gap follows the T^* line as a function of doping, but is at the same time associated to the “pair breaking” below T_c [13].

These considerations lead to a very strong phenomenology based on the phase fluctuations of the Cooper pairs, opening a channel for damping between T_c and T^* and giving a remarkable explanation for the filling of the AN spectral gap with temperature, up to T^* [46–52]. This theory was corroborated by the observation of an enormous Nernst effect going up to T^* in the Lanthanum and Bismuth compounds which was interpreted as the presence of vortices up to a very high temperature reaching very close to T^* [53–55].

A long controversy followed, in order to determine the extend of the temperature regime of phase fluctuations. Further experimental investigations, including Nernst effect on YBCO compounds [56]-where, contrarily to the LSCO compounds, the contribution of the quasi-particles has opposite sign from the contribution of the vortices, transport studies [57] and direct probing with Josephson SQUID experiments [58], led to the conclusion that, the phase fluctuations extend only a few tens of degrees above T_c but do not reach up to T^* . This issue can be resolved if we consider a competition of the SC phase fluctuations with fluctuations of a partner-competitor like particle-hole pairs, then it has been shown, through the study of a non linear σ -model (NL σ M) [59], that the true region of the SC phase fluctuations is reduced to a temperature window close to T_c . In the same line of thoughts, we examine here the possibility of extending fluctuations to a bigger symmetry group, where not only the phase of the Cooper pairs fluctuates but also there is a quantum superposition of Cooper pairs with a “partner-competitor” field.

2.1. Extended symmetry groups and the case for SU(2) symmetry

The idea to “rotate” the d-wave superconductor to another ‘partner’, hence enlarging the group allowed for

fluctuations is present in many theories for cuprates. A quick glance at the phase diagram of the cuprates would convince anyone that the most prominent features are the AF phase and the SC phase. Hence as a natural first guess, the rotation from the SC to the AF state has been tried, leading to an enlarged group of SO(5) symmetry [60–62]. The ten generators of the SO(5) group correspond to transitions between the various states inside the quintuplet (three magnetic states, and two SC states which are complex conjugate of one another). These theories are based on an underlying principle that the ‘partners’ are nearly degenerate in energy. The ‘partners’ possess an exact symmetry in the ground state in some nearby parameter regime, for example the SC and the AF states show exact degeneracy at half filling. At other parameters, the symmetry is realized only approximately in the ground state. The ‘hidden’ exact symmetry emerges when the system is perturbed from the ground state by increasing the temperature or the magnetic field. In the framework of emergent symmetries, the PG is created by fluctuations over a wide range of temperature. Later on, theories based on a SU(2) gauge structure in the pseudo spin space led the formation of flux phase [25], and rotation from the SC state to flux phases was envisioned. This theory had an emergent SU(2) symmetry with fluctuations acting as well up to temperatures T^* .

Recently, new developments have shown observation of charge modulations in the underdoped region of cuprate superconductors, in most of the compounds through various probes, starting with STM [9, 10], NMR [63, 64] and X-ray scattering [65–68]. At high applied magnetic field, the charge modulations reconstruct the Fermi surface, forming small electron pockets [69–76]. In YBCO, the charge modulations are stabilized as long range uniaxial $\mathbf{Q} = (Q_0, 0)$ 3D order above a certain magnetic threshold [77–79] and the thermodynamic lines can be determined with ultra-sound experiment [80, 81]. With the ubiquitous observation of charge modulations inside the PG phase, a rotation of the SC state towards a Charge Density Wave (CDW) state has been proposed [82–86]. This rotation has also two copies of an SU(2) symmetry group where one rotates the SC state to the real Δ_0^a and imaginary Δ_0^b parts of the particle-hole pair where (i, j) are sites on a bond (see Fig.3c) with $\mathbf{r}_j = \mathbf{r}_i \pm a_{x,y}$ and $\mathbf{r} = (\mathbf{r}_i + \mathbf{r}_j)/2$ and \mathbf{Q} is the modulation wave vector corresponding to the CDW state. In the case of the eight hot spots (EHS) model (defined after Eq. 6), \mathbf{Q} is the the diagonal wave vector $\mathbf{Q} = (Q_0, Q_0)$ (shown in Fig.3b) but experimentally, it is axial with $\mathbf{Q} = (0, Q_0)$ or $\mathbf{Q} = (Q_0, 0)$. We have the two $l = 1$ representations

$(\Delta_{-1}, \Delta_0, \Delta_1)$ with

$$\begin{aligned}\Delta_1 &= \frac{-1}{\sqrt{2}} \hat{d} \sum_{\sigma} \sigma c_{i\sigma}^{\dagger} c_{j-\sigma}^{\dagger} e^{i(\theta_i + \theta_j)}, \\ \Delta_0^a &= \frac{1}{2} \hat{d} \sum_{\sigma} \left[c_{i\sigma}^{\dagger} c_{j\sigma} e^{iQ \cdot r + i(\theta_i - \theta_j)} + c_{j\sigma}^{\dagger} c_{i\sigma} e^{-iQ \cdot r - i(\theta_i - \theta_j)} \right], \\ \Delta_0^b &= \frac{i}{2} \hat{d} \sum_{\sigma} \left[-c_{i\sigma}^{\dagger} c_{j\sigma} e^{iQ \cdot r + i(\theta_i - \theta_j)} + c_{j\sigma}^{\dagger} c_{i\sigma} e^{-iQ \cdot r - i(\theta_i - \theta_j)} \right], \\ \Delta_{-1} &= \frac{1}{\sqrt{2}} \hat{d} \sum_{\sigma} \sigma c_{j-\sigma} c_{i\sigma} e^{-i(\theta_i + \theta_j)}\end{aligned}\quad (4)$$

and the corresponding η - operators satisfy the SU(2) algebra,

$$\begin{aligned}[\eta_{\pm}, \Delta_m] &= \sqrt{l(l+1) - m(m \pm 1)} \Delta_{m \pm 1}, \\ [\eta_z, \Delta_m] &= m \Delta_m,\end{aligned}\quad (5)$$

with (note that η_z is identical for both representations a and b)

$$\begin{aligned}\eta_+^a &= \frac{1}{2} \sum_{\sigma} \sigma [c_{i\sigma}^{\dagger} c_{i-\sigma}^{\dagger} e^{iQ \cdot r} e^{2i\theta_i} + c_{j\sigma}^{\dagger} c_{j-\sigma}^{\dagger} e^{-iQ \cdot r} e^{2i\theta_j}], \\ \eta_-^a &= \frac{1}{2} \sum_{\sigma} \sigma [c_{i-\sigma} c_{i\sigma} e^{-iQ \cdot r} e^{-2i\theta_i} + c_{j-\sigma} c_{j\sigma} e^{iQ \cdot r} e^{-2i\theta_j}], \\ \eta_+^b &= \frac{i}{2} \sum_{\sigma} \sigma [-c_{i\sigma}^{\dagger} c_{i-\sigma}^{\dagger} e^{iQ \cdot r} e^{2i\theta_i} + c_{j\sigma}^{\dagger} c_{j-\sigma}^{\dagger} e^{-iQ \cdot r} e^{2i\theta_j}], \\ \eta_-^b &= \frac{-i}{2} \sum_{\sigma} \sigma [c_{i-\sigma} c_{i\sigma} e^{-iQ \cdot r} e^{-2i\theta_i} - c_{j-\sigma} c_{j\sigma} e^{iQ \cdot r} e^{-2i\theta_j}], \\ \eta_z &= \frac{1}{2} [\eta_+, \eta_-] = \frac{1}{2} \sum_{\sigma} (\hat{n}_{i\sigma} + \hat{n}_{j\sigma} - 1).\end{aligned}\quad (6)$$

An exact realization of the emergent symmetry has been found, where the Fermi surface is reduced to eight “hot spots” (crossing of the Fermi surface and the AF zone boundary as shown in Fig.3b) and the electrons interact with an AF critical mode in $d = 2$ [82–84, 87]. In this simple model, the gap equations could be solved showing the exact SU(2) symmetry between the Cooper pairing and particle-hole channels. We observed some ordering of a composite order parameter, which is a superposition of gaps in the particle-particle and particle-hole channels

$$\hat{\Delta}^* |0\rangle = \sum_{k\sigma} \left(c_{k\sigma}^{\dagger} c_{-k-\sigma}^{\dagger} + c_{k\sigma}^{\dagger} c_{k+Q\sigma} \right) |0\rangle, \quad (7)$$

where the modulations in the charge sector occur at a finite diagonal wave vector $\mathbf{Q} = (Q_x, Q_y)$, where Q_x and Q_y are the distance between two hot spots, as pictured in Fig.3b. A composite gap is formed at T^* with the mean square of the gaps in each channel

$$E^* = \sqrt{|\chi|^2 + |\Delta|^2}, \quad (8)$$

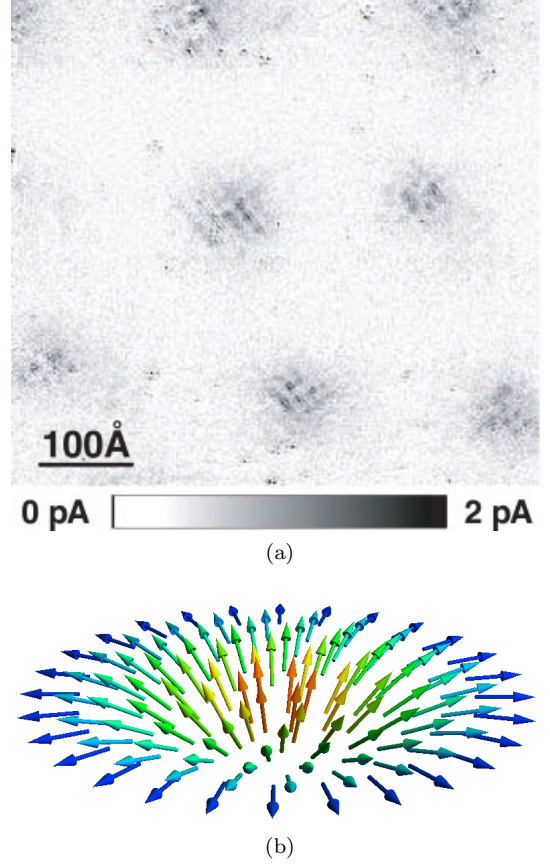


FIG. 4: a) Charge modulations observed in the vortex core, from the seminar paper [10]. The data were taken at magnetic field $B = 0T$ and $B = 8T$ and then subtracted. Charge modulations “appeared” inside the vortex core. b) Schematic picture of a Skyrmion in the η -space corresponding to the O(3) NL σ M in Eq.(15). The axes are (m_x, m_y, m_z) .

where χ is the gap in the particle-hole channel whereas Δ is the gap in the particle-particle channel.

Below T^* , a great amount of fluctuations are present which are described by the O(4) NL σ M [82, 88, 89]. For the four-fields $n_\alpha, \alpha = 1 \dots 4$, with $n_1 = (\Delta_{-1} + \Delta_1)/2$, $n_2 = (\Delta_{-1} - \Delta_1)/2$, $n_3 = \Delta_0^a$, $n_4 = \Delta_0^b$ the effective action writes

$$S = 1/2 \int d^d x \sum_{\alpha=1}^4 (\partial_\mu n_\alpha)^2, \quad \text{with} \quad \sum_{\alpha=1}^4 |n_\alpha|^2 = 1. \quad (9)$$

2.2. What can the model explain at this stage?

2.2.1. Charge modulations inside the vortex core

At this stage, the model can already explain a few properties of cuprate superconductors. Since the model treats very seriously the competition between CDW and SC pairing order parameters, it predicts charge modu-

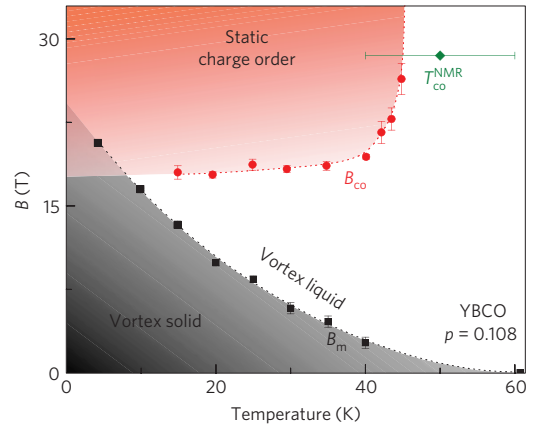
lations inside the vortex core (Fig.4a)[9–11, 63, 90]. Indeed, since the SC order parameter vanishes there, the competing order emerges at the core. The special structure associated to this feature is called a meron, or half skyrmion, in the pseudo-spin space. It can be noted that it is a generic prediction of the theories of emergent symmetries, that the competing order shows up inside the vortex core. For example, the SO(5) theory predicts AF correlations inside the vortex core [91, 92], whereas the SU(2) symmetry which rotates superconductivity to the π -flux phase predicts that the π -flux orbital state [16, 93] is present inside the vortex core. Although AF correlations were observed in the vortex core in the La-compounds [94], for YBCO, BSCCO and Hg-series, STM experiments [9, 10] and NMR [90] gave evidence for charge modulations. This ubiquitous observation of charge modulations inside the vortex core is a nice test for the theory of emergent SU(2) symmetry, but the presence of charge modulations inside the vortex core could also be explained by a strong competition between SC and CDW without invoking any emergent symmetry [95, 96].

2.2.2. B - T phase diagram

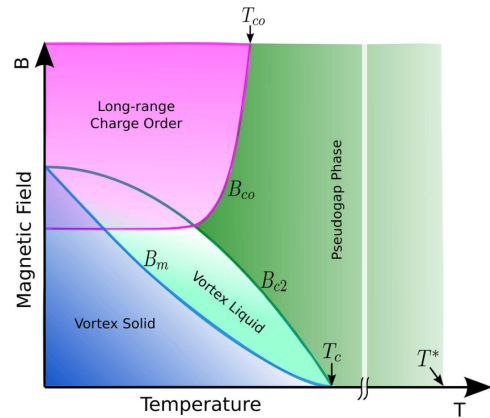
This leads us to a second set of experimental evidence, explicitly the phase diagram in the presence of an applied magnetic field as described in Figs.5a, 5b[35, 80]. For the compound YBCO, a phase diagram could be derived as a function of an applied magnetic field up to roughly $20T$. For this specific compound, one observes at $H_c = 17T$ [80], a second order phase transition towards a 3D charge order (CO) state with one uniaxial vector of modulations [77, 97]. The shape of this transition is very flat in temperature [80, 81], a fact that cannot be accounted by a simple model of competition between the two orders, but can be explained by a pseudo-spin flop transition, where the system suddenly goes from the SC state to the CO. The model of pseudo-spin flop comes directly from the expression of the $NL\sigma M$ where the constraint plays the role of the value of the spin in a magnetic spin-flop transition. The pseudo-spin flop transition accounts for the flatness [98] in temperature of the transition, but it does not explain the phase of co-existence [80, 90, 99]. Accounting for this phase requires to break the exact SU(2) symmetry underlying the $NL\sigma M$ by an amount of roughly 5%. As a conclusion, an SU(2) emergent symmetry and its $NL\sigma M$ can account for the whole phase diagram owing to the fact that it is broken by 5% [35].

2.2.3. Collective modes

An emergent symmetry is characterized by a set of collective modes [100]. Let us assume that the CDW is real, as in the first set of Eq.(4). Here the operators η and η^* which enable the “rotation” from the SC to the



(a)



(b)

FIG. 5: a) Experimental $B - T$ phase diagram from Ref.[80]. The shape of the lines is done with ultrasound experiments. b) Schematic phase diagram described through the SU(2) theory for competition between charge modulations and Cooper pairing [35].

CDW states are the generators of an O(3) Lie algebra

$$\mathcal{L} = \begin{pmatrix} 0 & * & * \\ -\frac{i}{2}(\eta_+^a - \eta_-^a) & 0 & * \\ -\eta_z & \frac{1}{2}(\eta_+^a + \eta_-^a) & 0 \end{pmatrix}, \quad (10)$$

where only the operator η^a in Eq.(6) contribute (since we rotate to the real part of the particle-hole pair), and where the notation $*$ stands for a hermitian matrix. The structure of \mathcal{L} in Eq.(10) give rise to collective modes. These collective modes are spin zero, charge two, and reflect the structure of the SU(2) symmetry. They can be considered as Pair Density Wave (PDW) excitations since they have non zero center of mass wave vector. They could be responsible for the mode observed in the A_{1g} channel in Raman Scattering [12] and can also be seen by spectroscopy experiments, like X ray, MEELS [101, 102] or soft X-rays [103], where the resolution in \mathbf{q} -space can be traced. The theory predicts that the mode occurs

around the same wave vector as the charge modulations and has a typical linear shape. Using the EHS model, we could fit the slope of the mode to a recent X-ray experiments on BSCCO compounds [103].

2.2.4. Symmetry of the spectral gap with respect to zero energy

The PG state is identified in various spectroscopies with either the pair-breaking peak as seen in the B_{1g} channel in Raman [104, 105], or the gap seen in STM [106] or ARPES [7, 107, 108]. The spectral “peak” or the gap concern the ANR of the Brillouin zone. One most noticeable feature about this gap is that it goes “unchanged” when one decreases the temperature to reach inside the SC phase [7, 107, 108]. Said in other words, the SC gap in the ANR below T_c remains the same when the temperature is raised up to T^* . This very unusual feature contrasts with the spectroscopic behavior around the node, as seen for example in the B_{2g} channel in Raman spectroscopy [104, 105], or in ARPES resolved in \mathbf{k} -space [108], where the gap as a function of temperature vanishes at T_c which is typical of a standard BCS behavior. The behavior in the ANR naturally calls for an interpretation in terms of the phase fluctuations of the SC pairing order parameter whereas the phase coherence sets up below T_c . This led to the development of a powerful phenomenology of the PG [109, 110], in which one distinguished feature is that the spectral gap is symmetric around $E = 0$ [20]. This feature is easily reproduced by any theory of preformed pairs and emergent symmetries. On the other hand, all other theories will produce an asymmetry of the PG around $E = 0$ (see e.g. Ref. [111–113]).

A somewhat related issue is the evolution of the number of carriers with doping, studied in a recent Hall measurement [114]. It is shown that the number of carriers evolves first linearly as the doping p , and then goes quite abruptly to $1 + p$, forming a large hole Fermi surface around the critical doping p^* . This behavior can be accounted by all the theories which open a gap around the eight hot spots (see Fig.3b), including theories coming from strong coupling scenarios [20, 115–117] or theories which open a gap on weaker coupling scenarios with standard symmetry breaking [20, 117, 118].

2.3. Microscopic models for emergent symmetries

A first generalization of the EHS model, was to start with a model for short range AF correlations, rather than a model of an AF QCP with critical fluctuations in 2D. A possible model consists of a simplification of the t-J model of Eq.(17), where the constraint of no double occupancy in the Gutzwiller projection operators [119] is treated at the mean-field level and where an extra nearest

neighbor (n.n.) Coulomb interaction is retained

$$H = \sum_{i,j,\sigma} t_{ij} (c_{i,\sigma}^\dagger c_{j,\sigma} + h.c) + \sum_{i,j} J_{i,j} \mathbf{S}_i \cdot \mathbf{S}_j + V_{i,j} n_i n_j, \quad (11)$$

where $c_{i,\sigma}^\dagger$ ($c_{i,\sigma}$) is a creation (annihilation) operator for an electron at site i with spin σ , $n_i = \sum_{\sigma} c_{i,\sigma}^\dagger c_{i,\sigma}$ is the number operator and $\mathbf{S}_i = c_{i,\alpha}^\dagger \boldsymbol{\sigma}_{\alpha,\beta} c_{i,\beta}$ is the spin operator at site i ($\boldsymbol{\sigma}$ is the vector of Pauli matrices). $J_{i,j}$ is an effective AF coupling which comes for example from the Anderson super-exchange mechanism [120]. The constraint of no double occupancy typical of the strong Coulomb onsite interaction is implemented through the Gutzwiller approximation by renormalizing the hopping parameter and the spin-spin interaction with $t(p) = g_t t = \frac{2p}{1+p} t$ and $J(p) = g_J J = \frac{4}{(1+p)^2} J$, where p is the hole doping while the density-density interaction is left invariant. We also assume that the AF correlations are dynamic, strongly renormalized, and short ranged, as given by the phenomenology of Neutron scattering studies for cuprates [121] and $V_{i,j}$ is a residual Coulomb interaction term.

The theory of the SU(2) emergent symmetry, although producing some strong phenomenology suffers from a few weaknesses. Maybe the most prominent one is the stability of the symmetry with respect to a small change of parameters in the model [122]. Let’s consider again the EHS model which has an exact realization of the symmetry. If we try to generalize to a real Fermi surface, we notice that the symmetry is valid only at the hot spots, but anywhere away in the Brillouin zone it is broken. In order to resolve this issue, we first enlarged the space of the charge modulations by considering multiple wave vectors depending on the position in \mathbf{k} -space. Although a bit artificial, this trick was developed in order to maximize the area in \mathbf{k} -space where the SU(2) symmetry is realized. The object thus created in the charge channel has the form of charge excitons and forms droplets in real space. This enabled us to have a theory for the proliferation of droplets in the under-doped region of cuprate superconductors [120, 123]. Formation of droplets, or phase separation in real space, is a very interesting idea to explain the PG region because it has been observed through NMR experiments that the PG phase is very robust with respect to induced disorder [22]. When a vacancy is induced in the compound, for example through Zn doping [2], or irradiation with electrons [124], most of the energy scales get powerfully reduced, like the SC T_c or the charge ordering temperature T_{co} , but the PG line remains unaffected. More precisely, NMR studies tell us that around the Zn- impurity a small region of AF correlations is forming, as if the close vicinity of the impurity was revealing the underlying presence of short range AF correlations. But in-between the Zn- impurities, we recover the unaffected PG. This tells us that

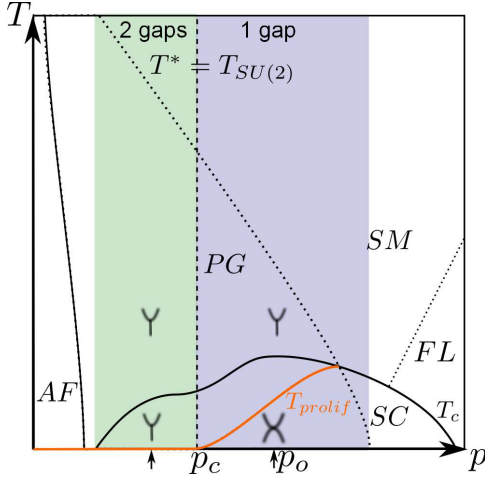


FIG. 6: Phase diagram for the Inelastic Neutron Scattering response at (π, π) from Ref.[126].

the PG is made of some short range “droplets” (in real space), which don’t “communicate” with one another, so that when a strong local perturbation is present (like the Zn - impurity) the PG is only affected locally [2, 125].

We identify two regimes as a function of doping (Fig. 6) [126]. At lower doping in the under-doped region ($0.06 < x < 0.12$) the droplets proliferate, which translates itself as a mixed character of the PG in the AN region with superposition of charge and SC gaps. This induces a special response in the Inelastic Neutron Scattering (INS), with the spin one mode observed at the AF wave vector (π, π) having a “Y” shape typical of the PG phase. The INS mode is treated in this theory as coming from spin excitons inside the SC phase or in the PG phase. On the other hand, at larger doping ($0.12 < x < 0.20$), the droplets become rarer and the gap in the ANR below T_c is a Cooper pair gap. In this region, the INS mode changes form below T_c with now an “hourglass” or typical “X” shape especially visible in the YBCO compound, where the splitting between the lower branches of the “X” coming from the border of the particle-hole continuum inside the SC phase (see [121] and reference therein).

The formulation of the SU(2) symmetry using multiple wave vectors was intended to preserve the symmetry in the ANR of the Brillouin zone. Although the possibility of multiple wave vectors is interesting, it is not very likely that a physical system does not choose one wave vector at least at lower temperature. Is there another route to get an organizing principle to treat the competition between the charge modulations and the SC without resorting to the multiple wave vectors trick?

3. PHASE TRANSITION AND HIGGS MECHANISM AT T^*

To summarize, in the last section, we gave an attempt of the generalization of the SU(2) symmetry for realistic Fermi surfaces and more realistic starting point of a model of short range AF interactions. The price we have to pay is to consider multiple wave vectors for the charge modulations. Although such a scenario is valid in theory, one could ask whether it is effectively realized in the experiments and whether we could get a more robust mechanism to get fluctuations at the T^* line.

3.1. Chiral model and Hopf mapping

A new idea came by noticing that the SU(2) symmetry that rotates the SC phase to the CDW modulations comes with two copies of SU(2) in the case (like in the EHS model) where the charge sector is a “bond exciton”- with a real and imaginary part [127]. As in the O(4) NL σ M Eq.(9), we have two complex operator fields

$$\begin{aligned} z_1 &= \hat{d} \sum_{\sigma} \sigma c_{j-\sigma} c_{i\sigma} \equiv \Delta_{ij}, \\ z_2 &= \hat{d} \sum_{\sigma} c_{i\sigma}^{\dagger} c_{j\sigma} e^{i\mathbf{Q} \cdot (\mathbf{r}_i + \mathbf{r}_j)/2} \equiv \chi_{ij}, \end{aligned} \quad (12)$$

with \hat{d} being the d-wave form factor and the constraint writes

$$E^* = \sqrt{|z_1|^2 + |z_2|^2}, \quad (13)$$

where E^* is a high energy scale which is interpreted as the PG energy scale in the case of the cuprate superconductors. Considering the spinor field $\psi = \begin{pmatrix} z_1 \\ z_2 \end{pmatrix}$, the constraint in Eq.(13) is invariant with respect to factorizing a global phase $\psi \rightarrow e^{i\theta} \psi$. This gauge invariance is visible in the SU(2) chiral model where the fields are allowed to fluctuate within an SU(2) matrix.

$$\begin{aligned} S &= \frac{1}{2} \int d^d x Tr [\partial_{\mu} \varphi^{\dagger} \partial_{\mu} \varphi], \quad \text{with } \varphi_{ab} = \frac{\delta_{ab}}{2} - z_a z_b^*, \\ &\text{and } \sum_{a=1}^2 z_a^* z_a = 1. \end{aligned} \quad (14)$$

Using the Hopf mapping of the sphere S_3 represented by Eq. (13) to the sphere S_2 , the model in Eq.(14) can be reduced to and O(3) NL σ M as follows (see a generic proof in [128]). We define $m^a = z_{\alpha}^* \sigma_{\alpha\beta}^a z_{\beta}$ where σ are Pauli matrices and the indices $a = x, y, z$, the effective action is now

$$S = 1/2 \int d^d x \sum_{a=1}^3 (\partial_{\mu} m^a)^2, \quad \text{with } \sum_{a=1}^3 |m^a|^2 = 1. \quad (15)$$

We see that the form in Eq.(15) is similar to the one of Eq.(9) but with three fields (O(3) NL σ M) rather than four (O(4) NL σ M). In the case of the two fields of Eq.(12) which represent the case of cuprates, the operators m_x , m_y and m_z correspond to PDW fluctuations.

3.2. $U(1) \times U(1)$ gauge theory and Higgs phase transition at T^*

The two complex fields Δ_{ij} and χ_{ij} in Eq. (12) are defined on bonds (i, j) with $\mathbf{r}_j = \mathbf{r}_i \pm a_{x,y}$ (see Fig.3c). Δ_{ij} and χ_{ij} represent preformed pairs in the particle-particle (PP) channel and the particle-hole (PH) channel. In order to construct a continuum field theory, these fields are defined on the midpoint of the bond, $\mathbf{r} = (\mathbf{r}_i + \mathbf{r}_j)/2$ such that $z_1(\mathbf{r}) = \Delta_{ij}$ and $z_2(\mathbf{r}) = \chi_{ij}$. The effective field theory will then have a $U(1) \times U(1)$ gauge structure. One $U(1)$ corresponds to the usual charge symmetry (usually broken by superconducting ground state) and the other is a consequence of the fact that we have pairs on bonds. By writing z_1 and z_2 on bonds, we have doubled the gauge structure to $U(1) \times U(1)$ with two gauge fields introduced in order to accommodate two independent phases. Without any loss of generality, the $U(1) \times U(1)$ gauge theory can be formulated in terms of a global and a relative phase of the two kinds of preformed pairs. In terms of the spinor ψ , the global and relative phases can be expressed as follows

$$\psi = e^{i\theta} e^{i\tau_3\varphi} \begin{pmatrix} \tilde{z}_1 \\ \tilde{z}_2 \end{pmatrix}, \quad (16)$$

where \tilde{z}_1 and \tilde{z}_2 are two fields which can carry d-wave symmetry and modulations. Typically here, $\tilde{z}_1 = \hat{d}|z_1|$ and $\tilde{z}_2 = \hat{d}|z_2|e^{i\mathbf{Q}\cdot\mathbf{r}}$. Two gauge fields a_μ and b_μ are introduced in the theory to enforce the gauge invariance. The transformation $\psi \rightarrow e^{i\theta} e^{i\tau_3\varphi}\psi$, $a_\mu \rightarrow a_\mu + \partial_\mu\theta$, $b_\mu \rightarrow b_\mu + \partial_\mu\varphi$ leaves the following action

$$\mathcal{S}_{a,b} = \int d^d x \left[\frac{1}{2g} |D_\mu\psi|^2 + V(\psi) + \frac{1}{4} F_{\mu\nu} F^{\mu\nu} + \frac{1}{4} \tilde{F}_{\mu\nu} \tilde{F}^{\mu\nu} \right], \quad (17)$$

with $D_\mu = \partial_\mu - ia_\mu - i\tau_3 b_\mu$,

$$F_{\mu\nu} = \partial_\mu a_\nu - \partial_\nu a_\mu,$$

$$\text{and } \tilde{F}_{\mu\nu} = \partial_\mu b_\nu - \partial_\nu b_\mu,$$

invariant, where τ_3 is the Pauli matrix in the spinorial space ψ and a_μ and b_μ are gauge fields corresponding respectively to the spinor's global phase θ and relative phase φ . A linear combination of the two gauge fields, $\mathbf{a} + \mathbf{b} = 2\mathbf{A}$ gives twice the electro-magnetic gauge field and another combination, $\mathbf{a} - \mathbf{b} = \tilde{\mathbf{a}}$ is identified as a dipolar field on a bond.

The concept of two kinds of preformed pairs and the resultant $U(1) \times U(1)$ gauge structure opens up unique possibilities with hierarchy of phenomenon occurring with reduction in temperature from a high value. At T^* , the system encounters a first Higgs mechanism

where the global $U(1)$ phase θ of the spinor ψ gets frozen. As a result, one gauge field acquires a mass $E^* = \sqrt{|\chi_{ij}|^2 + |\Delta_{ij}|^2}$ opening a gap in the ANR of the Brillouin zone and E^* characterizes the PG energy scale. Owing to this Higgs mechanism, the PG line will show universal features independent of the material specifics or disorder. Thus at T^* , the PP and PH pairs get entangled and compete strongly with each other. Due to this competition, both the amplitudes $|z_1|$ and $|z_2|$ fluctuate wildly along with fluctuations in the relative phase. The effective theory just below T^* corresponds to the O(3) NL σ M or, equivalently, to the SU(2) chiral model, and the typical excitations are made of PDW η -modes. The freezing of the global phase at T^* has removed one copy of the O(3) NL σ M leaving the other one untouched. It is to be noted that the O(3) NL σ M has topological excitations which are skyrmions in the pseudo-spin space and may account for the recently observed anomalous thermal Hall effect [129]. To explain the anomalous Hall effect, there are other recent proposals based on proximity to a quantum critical point of a 'semion' topological ordered state [130], presence of spin-dependent next-nearest neighbor hopping in the π -flux phase [131] or presence of large loops of currents [132]. If we continue to lower the temperature in the under-doped region, different temperature lines emerge (see Fig. 2). First, there are two cross-over mean-field lines corresponding to the condensation of the amplitudes of each field $\Delta_0(T) = |z_1|_0$ and $\chi_0(T) = |z_2|_0$, leading to a uniform d-wave Cooper pairing contribution below T_{fluc} and modulated d-wave charge contribution below T_{co} . Below each line, the preformed pairs have a non zero precursor gap in each channel, and these two channels compete. The two fields z_1 and z_2 still satisfy Eq. (13) with a condensed part (Δ_0 and χ_0) and a fluctuation part such that $|z_1| = \Delta_0(T) + \delta|z_1|$ and $|z_2| = \chi_0(T) + \delta|z_2|$. These lines do not have to be identical. In Fig.2 they are represented, with the first one T_{co} corresponding to a quasi long range charge order (experimentally this order is bi-dimensional, so that it is impossible to have it fully long range at finite temperature) and the second one T_{fluc} corresponding to the phase fluctuation regime of the Cooper pairs. Note that when $T_{fluc} < T_{co}$, a PDW composite order is induced below T_{fluc} , since the field $z_1 z_2 = \Delta\chi$ has the symmetry of a SC order with non-zero center of mass and its phase was frozen at T^* . These lines are determined by solving the gap equations in each channel, corresponding to the microscopic model in Eq.(11). Below T_c , the second freezing of the relative phase occurs and we are fully in the SC phase. One consequence of our theory, is that the SC ground state is actually a super-solid (or PDW), a fact that is supported by X-Ray experiments, which show that the charge order signal does not go to zero as $T \rightarrow 0$ in the SC phase (see e.g. [65]). Since our theory of preformed pairs is based on two complex fields, the phase in the particle-hole channel produces currents of d-density wave (dDW) [133] type, as well as a series of pre-emptive transitions

breaking C_4 symmetry (nematicity), time reversal symmetry (TR) and creating loop currents. The reasoning follows the steps of earlier works [134–136]. Another consequence of this double stage freezing of the phase is that the phase slip associated to the charge ordering is now stiff and related to the phase of the superconductor. This very unusual situation promises to open space for future experimental verifications.

3.3. What can this work explain?

The main idea of this work is to have two sets of preformed pairs, one in the particle-hole channel, that we called “bond excitons”, and one in the particle-particle channel—the Cooper pairs that become entangled at T^* . The freezing of the entropy down to $T = 0$ then follows its own route showing cascade of phenomenon occurring at different temperatures. The notion of preformed pairs shall be distinguished from the typical scenario of phase fluctuations [42, 48] around a mean field amplitude. Indeed, in the phase fluctuations scenario, the focus is put on the fluctuations only with no restrictions on the size of the pairs, whereas the preformed pair scenarios [50–52] put the accent on the very short size of the Cooper pair which opens a wide region in temperature where the pairs behave like a hard core boson and undergo Bose Einstein condensation. In view of the strong correlations in cuprates and the very short size of the Cooper pairs, the concept of preformed pairs is very natural. Moreover, recent experiments have revived the issue of fluctuating preformed pairs with their observation up to T^* in pump probe measurements [137–139] and in the over-doped region of the phase diagram in time domain spectroscopy [140]. We review below a few experiments which could be explained by such a scenario.

3.3.1. A precursor in the charge channel

A recent Raman scattering experiment performed on the compound Hg1223 shows for the first time that there is a precursor gap in the charge channel (see Fig.7a) [13]. It is seen as a spectral peak in the B_{2g} channel, which is visible below the ordering temperature T_{co} but follows T^* rather than T_{co} as a function of oxygen doping. This peak is attributed to charge modulations. The situation is very similar at what is observed in the AN region of the Brillouin zone. In the B_{1g} channel (which is scanning the AN region) a pair breaking peak is observed below T_c , but which follows T^* rather than T_c with doping. This spectral peak is also seen in ARPES [107, 108], where it is shown that it remains unchanged above T_c and just broadens through an additional source of damping [49, 108, 141], up to the PG temperature scale T^* . It is also seen in STM [106], at similar energy scales. A new feature of this very spectacular Raman scattering experiment is that it answers for the first

time to the question of whether charge modulations are “strong” or “weak” phenomenon in under-doped cuprates. Charge modulations have been seen in most of the compounds in the under-doped region, and although they are bi-dimensional, in theory they are “long range enough” to lead to a re-configuration of the Fermi surface observed through Quantum Oscillations (QO) [72]. But in this specific Raman experiment we see for the first time that the magnitude of the charge precursor gap in the B_{2g} channel is comparable to the magnitude of the Pair breaking gap in the B_{1g} channel, comforting the idea that the charge modulation is a “strong” effect in the physics of underdoped cuprates.

At this point, it is important to note that historically in the physics of cuprates, it is argued that there exists two energy scales corresponding to the PG phase (see e.g. the review [16]). First there is a higher energy scale associated with the depletion in the NMR Knight shift, referred to as the “Alloul-Warren” gap. This scale is also seen in Raman spectroscopies as a hump rather than a peak. Second scale corresponds to the spectroscopy peaks at a lower energy scale seen in STM, ARPES or Raman spectroscopy. Both the “Alloul-Warren” and the spectroscopic gaps seem to be related to each other and behave similarly with doping, decreasing in a quasi-linear fashion as doping increases[13]. The argument of two PG energy scales is typical of strong coupling theories where the higher energy scale is characterized with spin singlet formation and the lower energy scale is associated with superconducting fluctuations. In this work, the PG state is accompanied by a single energy scale E^* which is observed as spectroscopy peaks. The higher energy hump in Raman spectroscopy or the “Alloul-Warren” gap is not an independent energy scale and might be related to the coupling of fermions to a collective mode [142–144].

Using a BCS-like scaling argument for the different energy scales,

$$\begin{aligned}\chi &= 2\hbar\omega_c e^{-1/J_1\rho_0}, \\ \Delta &= 2\hbar\omega_c e^{-1/J_2\rho_0}, \\ E^* &= 2\hbar\omega_c e^{-1/J^*\rho_0}\end{aligned}\tag{18}$$

where the density of state at the Fermi level ρ_0 is taken to be constant, ω_c is the cut-off frequency of the interaction and $J^* = (J_1 + J_2)/2$, we can obtain their approximate doping dependence. The evolution of the energy scales with doping is shown on the right panel of Fig.7b where J_1 and J_2 have been chosen to be linearly decreasing with doping and vanish at two different doping p_1 and p_2 . In this simplified approach, E^* goes to zero at an intermediate doping p^* . We obtain the linear dependence of Δ and χ in an extended range of doping with $\Delta \approx \chi$ as observed in the Raman experiment Fig.7a. We also show that there exists only one PG energy scale $E^* \approx \Delta \approx \chi$. The concept of preformed pairs can then account, without resorting to the idea of a topological order, for the observation that upon application of a strong magnetic

field, the PG survives without a true $T = 0$ long range order [114]. Indeed around p^* application of a magnetic field up to 100T will certainly destroy SC phase coherence, but to destroy the pairs a much bigger field will be called for.

Our theory [127] addresses directly the formation of the spectral gaps χ and Δ which are visible in the B_{2g} and B_{1g} channels respectively

$$\Delta_{k,\omega} = -\frac{1}{\beta} \sum_{q,\Omega} \frac{J_-(q,\Omega) \Delta_{k+q}}{(\omega + \Omega)^2 - \xi_{k+q}^2 - \Delta_{k+q}^2}, \quad (19)$$

$$\chi_{k,\omega} = -\frac{1}{\beta} \sum_{q,\Omega} \frac{J_+(q,\Omega) \chi_{k+q}}{(\omega + \Omega - \xi_{k+q})(\omega + \Omega - \xi_{k+Q+q}) - \chi_{k+q}^2}.$$

with $J_{\pm}(q,\Omega)$ being related to the original model parameter as $J_{\pm}(q,\Omega) \sim 3J(p) \pm V$ and β is the inverse temperature. Solving Eq.(19) while keeping the momentum dependence of the gaps and allowing only one of them to be non-zero at each k-point we obtain the repartition shown in the left panel of Fig.7b. We see that the particle-particle pairing gap (yellow) is favored in the ANR while the particle-hole pairing gap (violet) prevails in the nodal region. This result agrees well with the Raman experiment where the SC pair-breaking peak appears in the B_{1g} symmetry which is probing the anti-nodal part of the Brillouin zone, while the precursor in the charge channel appears in the B_{2g} symmetry probing the nodal region. The PG energy scale is identified in the present theory as the scale at which the two preformed pairs start to get entangled and compete, $E^* = \sqrt{|\chi|^2 + |\Delta|^2}$, as first described in Eq.(13) for the case of the emergent SU(2) symmetry. Theories which can account for a precursor gap in the charge channel, which does not follow T_{co} but T^* with doping, and which is of the same size as the precursor gap in the Cooper channel, are very rare. This set of experiments, if confirmed, thus can be considered as a signature of a mechanism for two kinds of entangled preformed pairs. It has to be noted that the precursor in the charge channel has been seen, so far, only in the Hg1223 compound, where the three layers enhance the visibility of the charge channel. Similar findings were reported for YBCO but the analysis is more difficult due to the persistent noise in the B_{2g} channel.

3.3.2. Phase locking at T^*

The locking of the global phase of the two kinds of preformed pairs at T^* has serious experimental consequences. The PP and PH pairs become entangled at T^* and at lower temperatures T_c , the remaining relative phase is fixed. Now, if one applies an external magnetic field, it will create vortices where the SC order parameter will be suppressed. Inside each vortex the competing order parameter (in this case a bond excitonic order) is present, which typically occurs in theories with competing orders. A PDW order will be present in the vortex

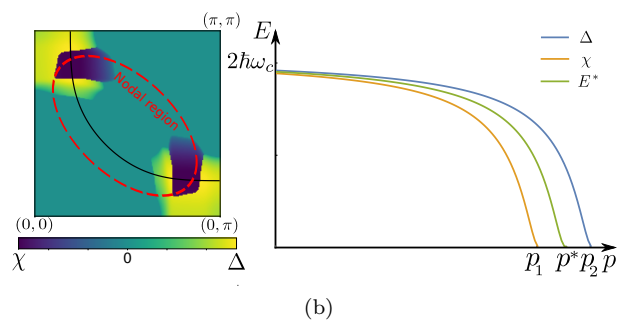
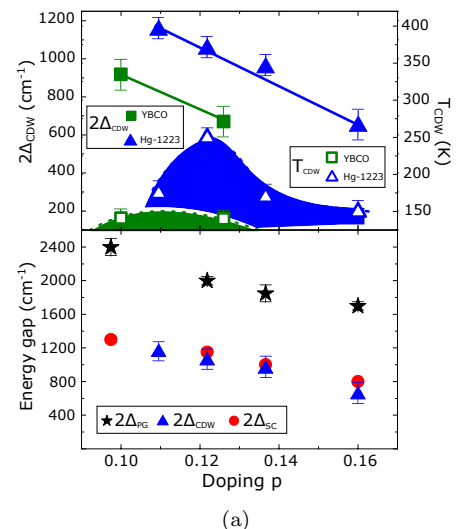


FIG. 7: a) Raman Scattering experiment [13] in Hg1223 where the two spectroscopic gaps in the B_{1g} (Cooper pairing called Δ_{SC} here) and B_{2g} (particle-hole pairing called Δ_{CDW} here) channels are shown to be of the same order or magnitude and to decrease linearly with doping like T^* . The higher energy hump Δ_{PG} also has the same doping dependence and is thus possibly not an independent energy scale. b) Theoretical solution of the gap equations Eq.(19) from the toy model Eq.(11). In the left hand side, a quarter of the Brillouin zone is represented with the Cooper pairing gap Δ in yellow and the preformed particle-hole gap χ in blue. Calculations are done for $T \geq T_c$. On the right hand side, the variation of the magnitude of the gap with doping is given, using a simplified BCS-like scaling argument.

halo [145–148]. But a stranger feature can be inferred by our theory. Since the phases of the Cooper pairs and the charge modulations have been locked at T^* , inside the vortices, the “phase-slip” of the charge modulations $\cos(\mathbf{Q} \cdot \mathbf{r} + \theta_r)$ is locked over a very long range $\langle \theta_r \rangle \neq 0$, longer than the typical size of each modulation patch, and thus much longer than the size of each vortex. This situation was observed in STM, where one sees that although there is a bit of spreading of the phase-slips around the mean value, the mean value itself is typically long range over the whole sample [149]. A concrete and strong ex-

perimental prediction would then naturally be to check the link between the patches of charge modulations and the SC phase. A Josephson-type of setup, where the SC phase is monitored through an applied current, would inevitably produce a correlation in the “phase-slips” of the charge modulations, a situation so unusual that, if verified, it would probably pin this theory to be the correct one.

3.3.3. $Q = 0$ orders at T^*

One of the great experimental complexity of the PG line, is that $\mathbf{Q} = 0$ orders have been observed around this line which break discrete symmetries. Loop currents observed through elastic neutron scattering [150], nematicity revealed through magneto-torque measurement [151, 152] and parity breaking observed via a second harmonic generation [153], all show a thermodynamic signature at T^* , the caveat being that $\mathbf{Q} = 0$ orders cannot open a gap in the electronic density of states. We are thus in a complex situation where the depletion of the density of states in the ANR cannot be explained by the $\mathbf{Q} = 0$ orders whereas any theory which gives an understanding of the PG will have to account for the presence of these intra unit cell orders at T^* .

The phase transition at T^* is of a very peculiar nature, with the freezing of the global phase of the spinor in Eq.(16) but also the opening of a gap it looks like a usual Higgs phenomenon. But the difference with the Meisner effect in a superconductor for example, is that the opening of the gap is made of a composite order rather than corresponding to the condensation of a simple field. The entanglement of two kinds of preformed pairs induces multiple orders in the PG phase. One can consider a composite field $\phi = \chi\Delta$ as a direct product of the two entangled fields. As the field ϕ correspond to particle-particle pairs with a finite center of mass momentum, this field has the same symmetries as that of a PDW field. Since ϕ has only a global phase and that it is frozen at T^* a global phase coherence sets up. But still, the field ϕ has huge fluctuations at T^* around a mean average $\langle\phi\rangle = \langle|\chi\Delta|e^{i\mathbf{Q}\cdot\mathbf{r}}\rangle$ in which the fluctuations of the amplitude might “wash out” the modulation term. The PDW field will condense to a long range order for temperatures below T_{fluc} where both the SC and the bond-excitonic orders obtain uniform components. One feature of this PDW is that its modulation wave vector will be same as that of the bond-excitonic order. Since we work with complex fields χ and Δ , the theory can potentially open auxiliary orders around T^* especially those, like loop currents or nematic order, which occur at $Q = 0$ but break a discrete symmetry Z_2 or C_4 . This situation has been described in previous works [135, 154], in particular in the case where T^* is identified with the formation of a long range PDW order [154] and where the second order magneto-electric tensor $l = |\phi_{\mathbf{Q}}|^2 - |\phi_{-\mathbf{Q}}|^2$ acquires a non zero value [155].

4. CONCLUSION

We have presented in this paper a review of our understanding of the PG phase of cuprate superconductors. This is an old problem, but which has generated a considerable amount of creativity in the last thirty years, both with theoretical concepts and with new experiments. We have put forward a scenario for the PG where a phase transition occurs at T^* where two kinds of preformed pairs, in the particle-hole and particle-particle channels, get entangled and start to compete. The effective model below T^* still retains a large amount of fluctuations, as is described as an $O(3)$ NL σ M, or equivalently the $SU(2)$ chiral model, which is reminiscent of theories of emergent symmetries with non abelian groups like the $SU(2)$ group. We stress that although the fluctuations below T^* belong to the same universality class as emergent symmetries, the new mechanism does not rely on the presence of an exact symmetry in the Lagrangian over the whole under-doped region. The gap opens in the ANR of the Brillouin zone due to the freezing of the global phase of our two kinds of preformed pairs. The model has a $U(1) \times U(1)$ gauge structure which enables to identify two phase transitions, one at T^* and another one at lower temperatures, at T_c . It has to be noted that models with $SU(2)$ gauge structure, both in the spin sector and the pseudo-spin sectors have been put forward recently to explain the PG though corresponding Higgs transitions at T^* .

The main difference between our approach and those models is that we do not “fractionalize” the electron at T^* into “spinon” and “holons” of some kinds. Instead, the electron keeps its full integrity, and the PG is due in our scenario to the entanglement of two kinds of preformed pairs in the charge and Cooper channels. The two approaches being antinomic, the future will tell whether one of the two is the right one (or whether maybe a third line of idea is needed). An argument in our favor lie in the recent observation of a precursor gap in the charge channel whose energy scale is related to the PG energy scale [13]. In consideration of the fractionalized scenario, it has been argued that there is some continuity between the PG at half filling and the PG in the under-doped region where the ground state is a superconductor, which would push the balance towards a fractionalized scenario for T^* (see e.g. [113] and references therein). We argue that “something” must happen at a doping of the order of $p \sim 0.05$ where numerous of “bond orders” sitting on the Oxygen atoms start to show up. Our intuition is that it is maybe the doping at which we lose the Zhang-Rice singlet [156], which thus liberates some degrees of freedom on the Oxygen atoms, leading to the formation of d-wave “bond” charge orders. At this stage it is just a speculation.

The scenario of entangled preformed pairs being simple enough, we hope that it will be possible to produce a strong predictive experiment in the near future.

This work has received financial support from

the ERC, under grant agreement AdG-694651-CHAMPAGNE. The authors also like to thank the

IIP (Natal, Brazil), for very inspirational visits, and for wonderful hospitality.

-
- [1] H. Alloul, T. Ohno, and P. Mendels, *Phys. Rev. Lett.* **63**, 1700 (1989).
- [2] H. Alloul, P. Mendels, H. Casalta, J. F. Marucco, and J. Arabski, *Phys. Rev. Lett.* **67**, 3140 (1991).
- [3] W. W. Warren et al., *Phys. Rev. Lett.* **62**, 1193 (1989).
- [4] J. C. Campuzano et al., *Nature* **392**, 157 (1998).
- [5] J. C. Campuzano et al., *Phys. Rev. Lett.* **83**, 3709 (1999).
- [6] K. M. Shen et al., *Science* **307**, 901 (2005).
- [7] I. M. Vishik et al., *New Journal of Physics* **12**, 105008 (2010).
- [8] I. M. Vishik et al., *Phys. Rev. Lett.* **104**, 207002 (2010).
- [9] W. D. Wise et al., *Nat. Phys.* **4**, 696 (2008).
- [10] J. E. Hoffman et al., *Science* **295**, 466 (2002).
- [11] M. H. Hamidian et al., *Nat. Phys.* **12**, 150 (2015).
- [12] S. Benhabib et al., *Phys. Rev. Lett.* **114**, 147001 (2015).
- [13] B. Loret et al., *Nature Physics*, 1 (2019).
- [14] B. Loret et al., *Physical Review B* **96**, 094525 (2017).
- [15] M. R. Norman and C. Pépin, *Rep. Prog. Phys.* **66**, 1547 (2003).
- [16] P. A. Lee, N. Nagaosa, and X.-G. Wen, *Rev. Mod. Phys.* **78**, 17 (2006).
- [17] A. Chubukov, D. Pines, and J. Schmalian, *J 2003 The Physics of Conventional and Unconventional Superconductors vol 1ed K.H. Bennemann and J. B. Ketterson*, Berlin:Springer, 2003.
- [18] T. M. Rice, K.-Y. Yang, and F. C. Zhang, *Reports on Progress in Physics* **75** (2012).
- [19] T. Senthil and P. A. Lee, *Phys. Rev. B* **79**, 245116 (2009).
- [20] S. Verret, O. Simard, M. Charlebois, D. Sénéchal, and A. M. S. Tremblay, *Physical Review B* **96**, 125139 (2017).
- [21] E. Fradkin, S. A. Kivelson, and J. M. Tranquada, *Rev. Mod. Phys.* **87**, 457 (2015).
- [22] H. Alloul, *Comptes Rendus Physique* **15**, 519 (2014).
- [23] D. J. Scalapino, *Numerical Studies of the 2D Hubbard Model*, in *Handbook of High-Temperature Superconductivity*, pages 495–526, Springer New York, New York, NY, 2007.
- [24] K. Le Hur and T. M. Rice, *Annals of Physics* **324**, 1452 (2009).
- [25] P. A. Lee, N. Nagaosa, T.-K. Ng, and X.-G. Wen, *Phys. Rev. B* **57**, 6003 (1998).
- [26] P. A. Lee and N. Nagaosa, *Phys. Rev. B* **46**, 5621 (1992).
- [27] G. Kotliar and J. Liu, *Phys. Rev. B* **38**, 5142 (1988).
- [28] T. Senthil and M. P. A. Fisher, *Physical Review B* **62**, 7850 (2000).
- [29] T. Senthil and M. P. A. Fisher, *Phys.Rev.Lett.* **86**, 292 (2001).
- [30] P. Lee and X.-G. Wen, *Phys. Rev. Lett.* **78**, 4111 (1997).
- [31] P. A. Lee, N. Nagaosa, T.-K. Ng, and X.-G. Wen, *Phys. Rev. B* **57**, 6003 (1998).
- [32] S. Sachdev, H. D. Scammell, M. S. Scheurer, and G. Tarnopolsky, *Phys. Rev. B* **99**, 054516 (2019).
- [33] A. Ferraz and E. Kochetov, *Nuclear Physics B* **853**, 710 (2011).
- [34] I. Ivantsov, A. Ferraz, and E. Kochetov, *Phys. Rev. B* **98**, 214511 (2018).
- [35] D. Chakraborty, C. Morice, and C. Pépin, *Phys. Rev. B* **97**, 214501 (2018).
- [36] G. Kotliar, *Phys. Rev. B* **37**, 3664 (1988).
- [37] P. W. Anderson, *Science* **235**, 1196 (1987).
- [38] P. W. Anderson et al., *J. Phys. Condens. Matter* **16**, R755 (2004).
- [39] T. Kloss, X. Montiel, V. S. de Carvalho, H. Freire, and C. Pépin, *Rep. Prog. Phys.* **79**, 084507 (2016).
- [40] Emery, V. J. and S. A. Kivelson, *Nature* **374**, 434 (1995).
- [41] L. Benfatto, S. Caprara, and C. D. Castro, *The European Physical Journal B - Condensed Matter and Complex Systems* **17**, 95 (2000).
- [42] L. Benfatto, C. Castellani, and T. Giamarchi, *Phys. Rev. Lett.* **98**, 117008 (2007).
- [43] Y. J. Uemura et al., *Phys. Rev. Lett.* **62**, 2317 (1989).
- [44] C. C. Homes et al., *Nature (London)* **430**, 539 (2004).
- [45] M. R. Norman, H. Ding, and M. Randeria, *J. Phys. Chem. Solids* **59**, 1902 (1998).
- [46] M. R. Norman, A. Kanigel, M. Randeria, U. Chatterjee, and J. C. Campuzano, *Phys. Rev. B* **76**, 174501 (2007).
- [47] M. R. Norman, M. Randeria, H. Ding, and J. C. Campuzano, *Phys. Rev. B* **52**, 615 (1995).
- [48] S. Banerjee, T. V. Ramakrishnan, and C. Dasgupta, *Phys. Rev. B* **83**, 024510 (2011).
- [49] S. Banerjee, T. V. Ramakrishnan, and C. Dasgupta, *Phys. Rev. B* **84**, 144525 (2011).
- [50] R. Boyack, C.-T. Wu, P. Scherpelz, and K. Levin, *Physical Review B* **90**, 220513 (2014).
- [51] R. Boyack, Q. Chen, A. A. Varlamov, and K. Levin, *arXiv.org*, 321 (2017).
- [52] C.-C. Chien, Y. He, Q. Chen, and K. Levin, *Physical Review B* **79**, 214527 (2009).
- [53] L. Li et al., *Phys. Rev. B* **81**, 054510 (2010).
- [54] L. Li, N. Alidoust, J. M. Tranquada, G. D. Gu, and N. P. Ong, *Phys. Rev. Lett.* **107**, 277001 (2011).
- [55] L. Li, Y. Wang, and N. P. Ong, *Phys. Rev. B*, 056502 (2013).
- [56] O. Cyr-Choiniere et al., *Physical Review B* **97**, 064502 (2018).
- [57] F. Rullier-Albenque, H. Alloul, and G. Rikken, *Phys. Rev. B* **84**, 014522 (2011).
- [58] N. Bergeal et al., *Nat. Phys.* **4**, 608 (2008).
- [59] G. Wachtel and D. Orgad, *Physical Review B* **90**, 224506 (2014).
- [60] E. Demler and S.-C. Zhang, *Phys. Rev. Lett.* **75**, 4126 (1995).
- [61] E. Demler, W. Hanke, and S.-C. Zhang, *Rev. Mod. Phys.* **76**, 909 (2004).
- [62] S.-C. Zhang, *Science* **275**, 1089 (1997).
- [63] T. Wu et al., *arXiv:1404.1617 [cond-mat.supr-con]* (2014).
- [64] T. Wu et al., *Nature* **477**, 191 (2011).

- [65] E. Blackburn et al., Phys. Rev. Lett. **110**, 137004 (2013).
- [66] S. Blanco-Canosa et al., Phys. Rev. Lett. **110**, 187001 (2013).
- [67] S. Blanco-Canosa et al., Phys. Rev. B **90**, 054513 (2014).
- [68] G. Ghiringhelli et al., Science **337**, 821 (2012).
- [69] N. Doiron-Leyraud et al., Nature **447**, 565 (2007).
- [70] D. LeBoeuf et al., Nature **450**, 533 (2007).
- [71] S. E. Sebastian et al., Phys. Rev. Lett. **108**, 196403 (2012).
- [72] W. Tabis et al., Nat. Commun. **5**, 5875 (2014).
- [73] N. Barišić et al., Nature Physics **9**, 761 (2013).
- [74] G. Grissonnanche and F. Laliberte, (2015).
- [75] F. Laliberté et al., Nat. Commun. **2**, 432 (2011).
- [76] J. Chang et al., Phys. Rev. Lett. **104**, 057005 (2010).
- [77] S. Gerber et al., Science **350**, 949 (2015).
- [78] J. Chang et al., Nat. Commun. **7** (2016).
- [79] H. Jang et al., Proc. Natl. Acad. Sci. **113**, 14645 (2016).
- [80] D. LeBoeuf et al., Nat. Phys. **9**, 79 (2013).
- [81] F. Laliberté et al., npj Quantum Materials **3**, 11 (2018).
- [82] K. B. Efetov, H. Meier, and C. Pépin, Nat. Phys. **9**, 442 (2013).
- [83] C. Pépin, V. S. de Carvalho, T. Kloss, and X. Montiel, Phys. Rev. B **90**, 195207 (2014).
- [84] M. A. Metlitski and S. Sachdev, Phys. Rev. B **82**, 075128 (2010).
- [85] W. A. Atkinson, A. P. Kampf, and S. Bulut, New J. Phys. **17**, 013025 (2015).
- [86] H. Freire, V. S. de Carvalho, and C. Pépin, Phys. Rev. B **92**, 045132 (2015).
- [87] A. Abanov, A. V. Chubukov, and J. Schmalian, Adv. Phys. **52**, 119 (2003).
- [88] M. Eimenkel, H. Meier, C. Pépin, and K. B. Efetov, Phys. Rev. B **90**, 054511 (2014).
- [89] L. E. Hayward, D. G. Hawthorn, R. G. Melko, and S. Sachdev, Science **343**, 1336 (2014).
- [90] T. Wu et al., Nat. Commun. **4**, 2113 (2013).
- [91] D. P. Arovas, A. J. Berlinsky, C. Kallin, and S.-C. Zhang, Phys. Rev. Lett. **79**, 2871 (1997).
- [92] A. Ghosal, C. Kallin, and A. J. Berlinsky, Phys. Rev. B **66**, 214502 (2002).
- [93] P. A. Lee and X.-G. Wen, Phys. Rev. B **63**, 224517 (2001).
- [94] B. Lake et al., Science **291**, 1759 (2001).
- [95] S. A. Kivelson, D.-H. Lee, E. Fradkin, and V. Oganesyan, Phys. Rev. B **66**, 144516 (2002).
- [96] Y. Zhang, E. Demler, and S. Sachdev, Phys. Rev. B **66**, 094501 (2002).
- [97] J. Chang et al., Nat. Commun. **7**, 11494 (2016).
- [98] H. Meier, M. Eimenkel, C. Pépin, and K. B. Efetov, Phys. Rev. B **88**, 020506 (2013).
- [99] J. Kačmarčík et al., Phys. Rev. Lett. **121**, 167002 (2018).
- [100] C. Morice, D. Chakraborty, and C. Pépin, Phys. Rev. B **98**, 224514 (2018).
- [101] S. Vig et al., SciPost Physics **3**, 026 (2017).
- [102] M. Mitrano et al., Proceedings of the National Academy of Sciences **115**, 5392 (2018).
- [103] L. Chaix et al., Nature Physics **13**, 952 (2017).
- [104] A. Sacuto et al., Reports on Progress in Physics **76**, 022502 (2013).
- [105] T. P. Devereaux and R. Hackl, Rev. Mod. Phys. **79**, 175 (2007).
- [106] M. Kugler, O. Fischer, C. Renner, S. Ono, and Y. Ando, Phys. Rev. Lett. **86**, 4911 (2001).
- [107] A. Damascelli, Z. Hussain, and Z.-X. Shen, Rev. Mod. Phys. **75**, 473 (2003).
- [108] I. M. Vishik, Reports on Progress in Physics **81**, 062501 (2018).
- [109] P. A. Lee, Phys. Rev. X **4**, 031017 (2014).
- [110] X. Montiel, T. Kloss, and C. Pépin, EPL (Europhysics Letters) **115**, 57001 (2016).
- [111] W. Wu et al., Phys. Rev. X **8**, 021048 (2018).
- [112] S. Sakai, M. Civelli, and M. Imada, Phys. Rev. Lett. **116**, 057003 (2016).
- [113] S. Sakai, M. Civelli, and M. Imada, Physical Review B **98**, 195109 (2018).
- [114] S. Badoux et al., Nature (London) **531**, 210 (2016).
- [115] K.-Y. Yang, T. M. Rice, and F.-C. Zhang, Phys. Rev. B **73** (2006).
- [116] S. Chatterjee, S. Sachdev, and A. Eberlein, Phys. Rev. B **96**, 075103 (2017).
- [117] J. G. Storey, EPL (Europhysics Letters) **113**, 27003 (2016).
- [118] C. Morice, X. Montiel, and C. Pépin, Physical Review B **96**, 134511 (2017).
- [119] A. Paramekanti, M. Randeria, and N. Trivedi, Phys. Rev. Lett. **87**, 217002 (2001).
- [120] X. Montiel, T. Kloss, and C. Pépin, Phys. Rev. B **95**, 104510 (2017).
- [121] V. Hinkov et al., Nat. Phys. **3**, 780 (2007).
- [122] X. Wang, Y. Wang, Y. Schattner, E. Berg, and R. M. Fernandes, Phys. Rev. Lett. **120**, 247002 (2018).
- [123] X. Montiel, T. Kloss, and C. Pépin, Scientific Reports **7**, 3477 (2017).
- [124] F. Rullier-Albenque et al., EuroPhys. Lett. **50**, 81 (2000).
- [125] H. Alloul, J. Bobroff, M. Gabay, and P. J. Hirschfeld, Rev. Mod. Phys. **81**, 45 (2009).
- [126] X. Montiel and C. Pépin, Phys. Rev. B **96**, 094529 (2017).
- [127] D. Chakraborty et al., arXiv e-prints , arXiv:1906.01633 (2019).
- [128] E. Fradkin, **Field theories of condensed matter systems** , in *Field theories of condensed matter systems*, page see chap.7.9, Sarat Book House, 2007.
- [129] G. Grissonnanche et al., arXiv e-prints , arXiv:1901.03104 (2019).
- [130] S. Chatterjee et al., arXiv e-prints , arXiv:1903.01992 (2019).
- [131] J. H. Han, J.-H. Park, and P. A. Lee, arXiv e-prints , arXiv:1903.01125 (2019).
- [132] C. M. Varma, arXiv e-prints , arXiv:1903.04699 (2019).
- [133] S. Chakravarty, R. B. Laughlin, D. K. Morr, and C. Nayak, Phys. Rev. B **63**, 094503 (2001).
- [134] Y. Wang and A. Chubukov, Phys. Rev. B **90**, 035149 (2014).
- [135] Y. Wang, D. F. Agterberg, and A. Chubukov, Phys. Rev. B **91**, 115103 (2015).
- [136] Y. Wang, D. F. Agterberg, and A. Chubukov, Phys. Rev. Lett. **114**, 197001 (2015).
- [137] S. Rajasekaran et al., Science **359**, 575 (2018).
- [138] W. Hu et al., Nature Materials **13**, 705 (2014).
- [139] D. Fausti et al., Science **331**, 189 (2011).
- [140] F. Mahmood, X. He, I. Božović, and N. P. Armitage, Phys. Rev. Lett. **122**, 027003 (2019).
- [141] M. R. Norman, M. Randeria, H. Ding, and J. C. Cam-

- puzano, Phys. Rev. B **57**, R11093 (1998).
- [142] M. Eschrig and M. R. Norman, Phys. Rev. Lett. **85**, 3261 (2000).
- [143] M. Eschrig, Advances in Physics **55**, 47 (2006).
- [144] A. Chubukov, T. Devereaux, and M. Klein, Phys. Rev. B **73**, 094512 (2006).
- [145] M. H. Hamidian et al., Nature **532**, 343 (2016).
- [146] S. D. Edkins et al., arXiv e-prints , arXiv:1802.04673 (2018).
- [147] Y. Wang et al., Phys. Rev. B **97**, 174510 (2018).
- [148] Z. Dai, Y.-H. Zhang, T. Senthil, and P. A. Lee, Phys. Rev. B **97**, 174511 (2018).
- [149] M. H. Hamidian et al., arXiv e-prints , arXiv:1508.00620 (2015).
- [150] B. Fauqué et al., Phys. Rev. Lett. **96**, 197001 (2006).
- [151] Y. Sato et al., Nature Physics **13**, 1074 (2017).
- [152] H. Murayama et al., arXiv e-prints , arXiv:1805.00276 (2018).
- [153] L. Zhao et al., Nat. Phys. **13**, 250 (2016).
- [154] D. F. Agterberg, D. S. Melchert, and M. K. Kashyap, Phys. Rev. B **91**, 054502 (2015).
- [155] S. Sarkar, D. Chakraborty, and C. Pépin, arXiv e-prints , arXiv:1906.08280 (2019).
- [156] F. C. Zhang and T. M. Rice, Phys. Rev. B **37**, 3759 (1988).